CHARACTERIZING A TWO-CHANNEL PHOSWICH DETECTOR USING RADIOXENON ISOTOPES PRODUCED IN THE OREGON STATE UNIVERSITY TRIGA REACTOR

Abi T. Farsoni and David M. Hamby

Oregon State University

Sponsored by the National Nuclear Security Administration

Award No. DE-FC52-06NA27322
Proposal No. BAA06-36

ABSTRACT

Low concentrations of radioxenon isotopes can be measured with a high sensitivity using beta/gamma coincidence technique. In this technique, a coincidence event is recorded when two signals from beta and gamma detection channels are detected simultaneously. These two coincident signals are then processed to establish a two-dimensional beta/gamma coincidence spectrum in which the four radioxenon isotopes can be measured in the sample. In many beta/gamma coincidence systems, beta and gamma radiations are detected in two separate channels. Another approach is to use a phoswich detector in which both radiations can be detected by one single channel, and simplifying the coincidence system configuration.

To expand the solid angle of the radioxenon detection geometry close to 4π, a two-channel and planar triple-layer phoswich detection system was designed and constructed. In order to characterize the phoswich detection system for radioxenon measurements, we have irradiated enriched stable samples of ^{132}Xe and ^{134}Xe gas with thermal neutrons from the TRIGA reactor at the Oregon State University (OSU). ^{133m}Xe, ^{133}Xe, and ^{135}Xe were successfully produced and injected into the detector gas cell using a simple gas transfer manifold system. To enhance the efficiency of coincidence detection between the two phoswich detectors, a synchronization logic mode was added into the previous firmware of our two-channel digital pulse processor system. In this paper, we will describe xenon neutron irradiation conditions, sample transfer procedures, and beta/gamma coincidence measurements results. Also a brief description of our synchronization logic mode will be covered in this paper.

OBJECTIVE

The Comprehensive Nuclear-Test-Ban Treaty Organization (CTBTO) has established the International Monitoring System (IMS) to monitor underground nuclear weapon tests by several verification means including measuring the concentration of radioactive xenon gas in the atmosphere. Several high-performance detection systems have been developed or are under development to detect the four radioxenon (^{131m}Xe, ^{133m}Xe, ^{133}Xe and ^{135}Xe) in the atmosphere. The Swedish Automatic Unit for Noble gas Acquisition (SAUNA, Ringbom et al., 2003), the SPALAX unit (Fontaine et al., 2004) and Automated Radioxenon Sampler and Analyzer (ARSA, McIntyre et al., 2001) are among these detection systems. Except for the SPLAX unit which uses a high-purity germanium detector to detect only X-rays and gamma-rays, other systems are designed based on beta/gamma coincidence measurement techniques in which both beta particles (or conversion electrons) and gamma-rays (or X-ray) must be detected simultaneously. Albeit with different geometry designs, both the SAUNA and the ARSA systems use two separate scintillation channels for detecting beta-particles and gamma-rays. Since the two scintillation channels in the SAUNA and ARSA systems are optically isolated from each other, scintillation photons are collected with more than one photomultiplier tube (PMT) for each channel. In the SAUNA system, three PMT's are used to detect a coincidence event: two PMT's in the beta channel and one PMT in the gamma channel. In the ARSA system, four PMT's are involved in detecting a coincidence event for each gas cell: two PMT's in the beta channel and two PMT's in the gamma channel.

Beta/gamma coincidence detection can be simplified using phoswich detectors in which both beta-particles and gamma-rays can be detected simultaneously using a single PMT (Ely et al., 2003; Hennig et al., 2005; Farsoni et al., 2007). In phoswich detectors, more than one scintillation material is optically coupled to a PMT. Beta/gamma coincidence events then can be identified using digital pulse shape analysis of the anode pulses. We have developed a two-channel phoswich detection system based on our single-channel prototype phoswich detector (Farsoni et al., 2009). Each phoswich detector consists of three scintillation layers: BC-400, CaF_2 and NaI(Tl) to detect beta-particles (CE), X-rays and gamma-rays, respectively. We have also developed and constructed a two-channel, fast and compact digital pulse processor to capture and analyze complicated anode pulses from the two-channel phoswich detector. The digital pulse processor captures anode pulses with a maximum sampling rate of 250 MHz and an amplitude resolution of 12 bits independently from each channel. All the digital modules and functions such as trigger logic, circular buffer and coincidence detection are implemented in a 1500K gate-equivalent SPARTAN-3 field-programmable gate array (FPGA) from Xilinx Incorporated. The on-board FPGA is automatically programmed via a high-speed USB2.0 port when the processor is connected to the personal computer (PC). Once the FPGA is programmed, the high-speed USB2.0 interface is used either for controlling the processor or transferring data. In this paper, we will present our recent measurements with xenon radioisotopes produced in the TRIGA reactor at the Oregon State University. We also describe our simple procedure to transfer stable and irradiated xenon gas from its vessel to reactor and from there to the detector gas cell. To enhance the coincidence efficiency of the two-channel system, a synchronizing mode was designed and added into the original firmware of the FPGA deployed on the digital pulse processor, a brief description of this mode in capturing coincidence events between the two channel will be presented as well.

RESEARCH ACCOMPLISHED

Detector Design

Based on our previous experiments with a prototype phoswich detector (Farsoni et al., 2009), a two-channel phoswich detection system was designed and constructed. The detector consists of a thin hollow disk (with 2 mm thickness and 76.2 mm diameter) as xenon gas cell, surrounded by two identical planar triple-layer phoswich detectors (Figure 1). The gas cell is completed by an aluminum sleeve which also joins the two detectors (Figure 2). This design provides a solid angle of about 3.4π for the gas cell, close to that of the ARSA system (~ 3.5π). The planar shape of the detectors has several important advantages, among which are the reduced cost due to its simplicity, and because it has a minimum non-uniformity in light collection efficiency, will not unreasonably degrade the beta or gamma energy resolution. Each phoswich detector consists of a plastic scintillator (1.5 mm) for detecting beta and conversion electrons, a CaF_2 crystal (2.0 mm) for X-ray detection and a NaI(Tl) crystal (25.4 mm) for measuring gamma rays.

Previous tests on the ARSA system have shown that latent radioxenon remains in the gas cells even after evacuation of the gases, leading to a memory effect which increases the background level for subsequent measurements.

Research performed at the Pacific Northwest National Laboratory (Seifert et al., 2005) showed that use of a 1-µm aluminum layer on plastic scintillators affectively reduces the memory effect from radioxenon gases remaining in the cells after evacuation. Therefore, to minimize this effect, a very thin layer of aluminum (1 µm) was deposited on the surface of two plastic scintillators (facing the gas cell). The aluminum coating process was performed using vacuum coating process at the Oregon State University. The coated plastic scintillators then were sent to the Saint-Gobain company for final assembly of the phoswich detectors. In addition, the aluminum coating on each plastic scintillator will optically isolate the two phoswich detectors from each other and make a reflection surface for each detector.

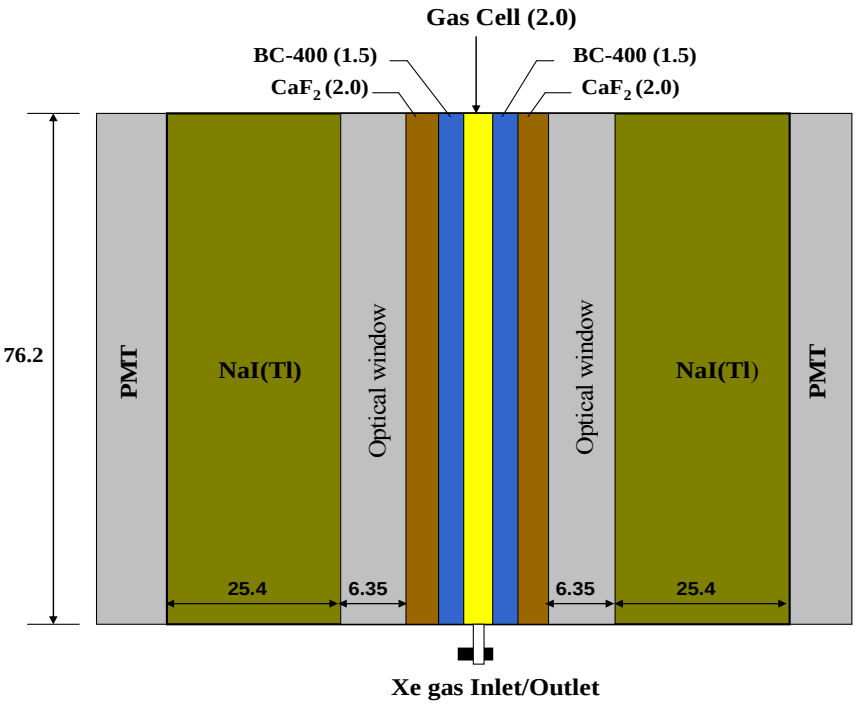

Figure 1. Schematic arrangement of the two-channel phoswich detector. All dimensions are in millimeters.

Radioxenon Production

To characterize our phoswich detectors in measuring xenon radioisotopes, two enriched (> 99%) and stable isotopes of xenon, ^{132}Xe and ^{134}Xe, were purchased. These stable xenon isotopes were activated by thermal neutrons in our TRIGA reactor at the Oregon State University to produce ^{133m}Xe, ^{133}Xe and ^{135}Xe. Our calculations show that irradiating 3 ml of these stable xenon isotopes in a thermal flux of $7x10^{10}$ n . cm^{-2}. sec^{-1} (in the thermal column of the TRIGA reactor) for 30 minutes generates 0.05 µCi of ^{133m}Xe, 0.17 µCi of ^{133}Xe and 1.47 µCi of ^{135}Xe.

Gas Transfer Manifold System

Designing a simple but efficient way to irradiate a small amount of xenon gas was essential for our radioxenon production and measurement work. The simplest way was to use a disposable syringe as a gas irradiation chamber. Polypropylene syringes mainly contain hydrocarbons and do not produce significant activity after neutron irradiation. Then, a low-cost gas transfer manifold system was designed to transfer gas from its cylinder to a disposable polypropylene syringe and from there to the detector gas cell (after neutron activation). The manifold system consists of a vacuum pump, a plastic Luer manifold and polyethylene pipes as depicted in Figure 2. This very simple but handy and efficient arrangement transfers the stable xenon gas from its vessel into a 3 ml disposable polypropylene syringe. The syringe, containing stable xenon, is then irradiated in the thermal column of OSU's

TRIGA reactor. The activated xenon gas is then injected into the phoswich detector using the same manifold as depicted in Figure 2.

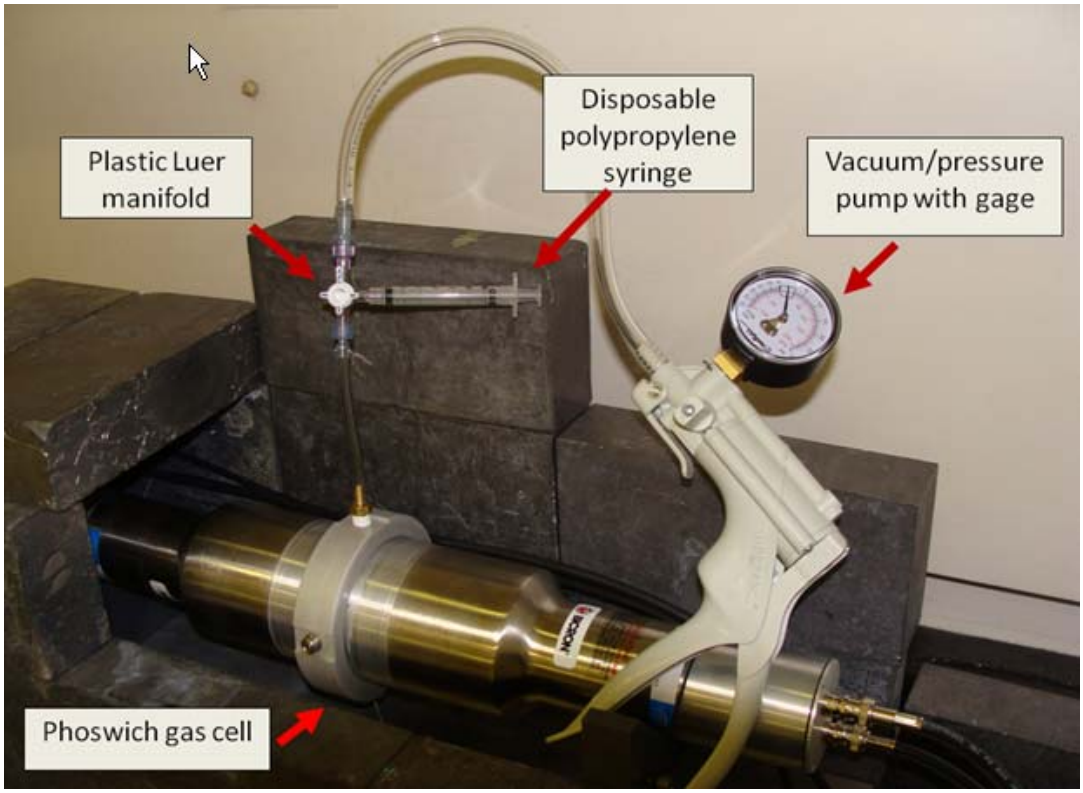

Figure 2. Manifold arrangement to transfer radioactive xenon gas from syringe into the detector gas cell.

Synchronizing Mode

To identify and capture coincidence events between the two channels, instead of using the time stamp method, a coincidence state machine was designed and added into the current FPGA firmware. When two channels are triggered in a predefined coincidence window, those pulses are tagged as coincidence pulses, otherwise as singles. Also for prototyping proposes and to have more flexibility in analyzing anode pulses from the two detectors, all the signal processing analysis are implemented in the PC side. Thus valid pulses from each detector are captured in the digital processor, tagged as either coincidence or single and are uploaded to the PC via high-speed USB interface for further analysis. In high-count rates, when the average time between two events is much less than the USB uploading time, most of the time one channel is waiting to be uploaded while the other channel is ready to be triggered and therefore a small fraction of coincidence events can be practically captured. Obviously, this will reduce the efficiency of our digital processor in capturing coincidence pulses between the two detectors.

To improve the efficiency of capturing coincidence events, the coincidence state machine was designed to work in two modes: (1) Free-Running or (2) Synchronizing modes. In the Free-Running mode, both channels freely and independently can make a trigger for the system. In the Synchronizing mode, however, any channel can be a trigger when the other channel is ready to get triggered (e.g., not being in a wait state for uploading the pulse data to the PC). In very low-count rates, both modes perform similar functionality in terms of capturing coincidence events between the two detectors. In the Synchronizing mode, any free channel will wait until the other channel exits the wait state then is ready to get triggered, making both channels synchronized in capturing coincidence events. Our experimental results using ^{133}Xe confirmed higher coincidence efficiency for high-count rates when using the Synchronizing mode.

To obtain an optimum coincidence window in the Synchronizing mode, ^{133}Xe was injected into the gas cell and the percentage of coincidence events versus coincidence window was recorded. The results of this experiment are

shown in Figure 3. Since the coincidence state machine in the FPGA is clocked with a frequency of 200 MHz (same as the analog-to-digital converter sampling rate), the time resolution for the coincidence window is one clock period or 5 nsec. Zero value for the coincidence window in Figure 3 is referred to capturing the coincidence event in the same clock period. By increasing the coincidence window up to a 9 clock period or 45 nsec, the coincidence percentage increases linearly. After then, it reaches a semi-flat region where we believe any increase in coincidence percentage is a result of random coincidences. Therefore, we decided to set the coincidence window at a 10 clock period or 50 nsec for the rest of experiments as indicated with a vertical and green dashed line in Figure 3. In this experiment, using the Free-Running mode and the coincidence window set at 50 nsec, only 0.68% of events were recorded as coincidence events.

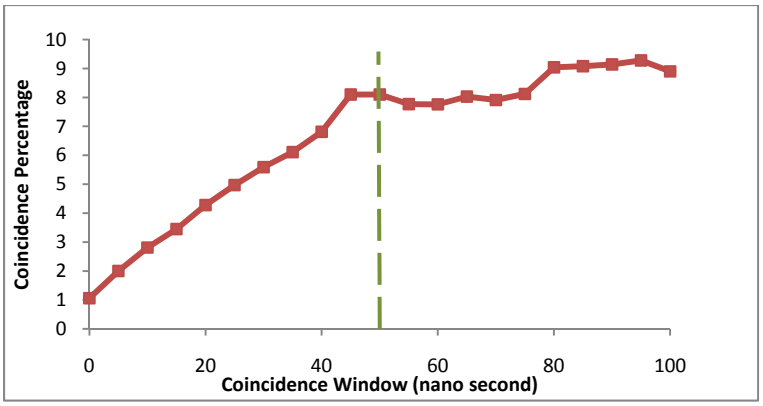

Figure 3. Coincidence percentage between two phoswich detectors versus coincidence window recorded using the Synchronizing mode when ^{133}Xe was injected into the gas cell.

Experimental Results

To minimize the ringing effect (Farsoni et al., 2009), the detector supplier (Saint-Gobain) suggested the replacement of the previous PMT (ET 9305B) with one with a better timing performance (ET 9821B). Before starting our measurements with xenon radioisotopes, the response of two phoswich detectors were examined using radioactive lab sources. For purpose of gain matching, the high voltage for phoswich detectors 1 and 2 was set to 1550 and 1450 V, respectively. Although not completely eliminated, the new detectors still showed a small ringing effect when detectors generate fast pulses from the plastic scintillators. For this reason, correction factors were used in our pulse processing analysis to correct pulse integration when a fast component appeared in the anode pulses.

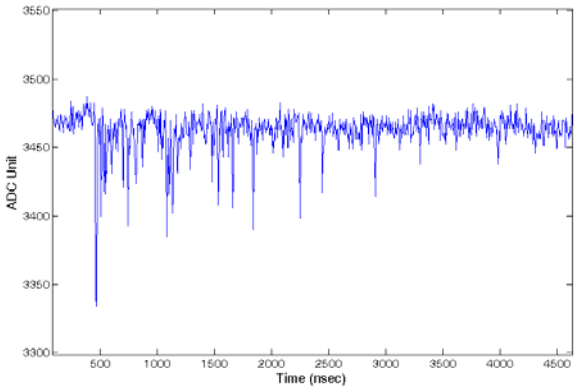

Figure 4. A typical anode pulse when a 30 keV X-ray is absorbed in the CaF_2 crystal.

Comparing to our prototype detector, the new detectors showed lower anode pulse heights (with the same energy deposition at nominal PMT voltages). This affects our pulse shape discrimination analysis, particularly for identifying and measuring 30 keV X-rays from ^{133}Xe and ^{133m}Xe. As mentioned before, pulses from CaF_2 crystal are selectively analyzed to measure the 30 keV X-rays. Regarding the fact that the CaF_2 crystal has a relatively low light yield, this makes the corresponding pulses very close to the noise level and difficult to detect and analyze. To discriminate 30 keV pulses from the noise, the trigger filter used in the FPGA was replaced with a longer filter (150 nsec peaking time). A typical anode pulse from 30 keV X-ray absorbed in CaF_2 crystal, when the phoswich detector was exposed to ^{133}Xe, is shown in Figure 4. This figure shows that the pulse has lost its slow decay shape and instead spikes from single scintillation photons have appeared. This might be due to either low light collection efficiency or low PMT quantum efficiency. We investigated possible relation between the aluminum coating and the light collection efficiency by examining the corresponding channel number of 662 keV photopeak from ^{137}Cs while the source was placed in different positions around the detector. These tests were repeated with a reflective mylar layer attached on the detector's front window (plastic scintillator). No significant differences in the channel number of 662 keV were observed through these experiments.

^{135}Xe measurements

To produce ^{135}Xe, 3 ml of enriched and stable ^{134}Xe was irradiated in the thermal column of the TRIGA reactor for 30 minutes. The thermal neutron flux for this irradiation was $7x10^{10}$ n.cm^{-2}.sec^{-1}. The resulting radioxenon activity was calculated to be around 1.47 µCi. Then, using the gas transfer manifold (Figure 2), activated xenon gas was injected into the detector gas cell about 24 hours after the neutron irradiation. Using our high-speed two-channel digital processor (Farsoni et al., 2008), about three million anode pulses were recorded for off-line digital pulse processing. 2-D beta-gamma coincidence energy spectra from ^{135}Xe in each phoswich detectors are shown in Figure 5. Horizontal and vertical axis in this figure represent energy absorption in BC-400 and NaI(Tl), respectively.

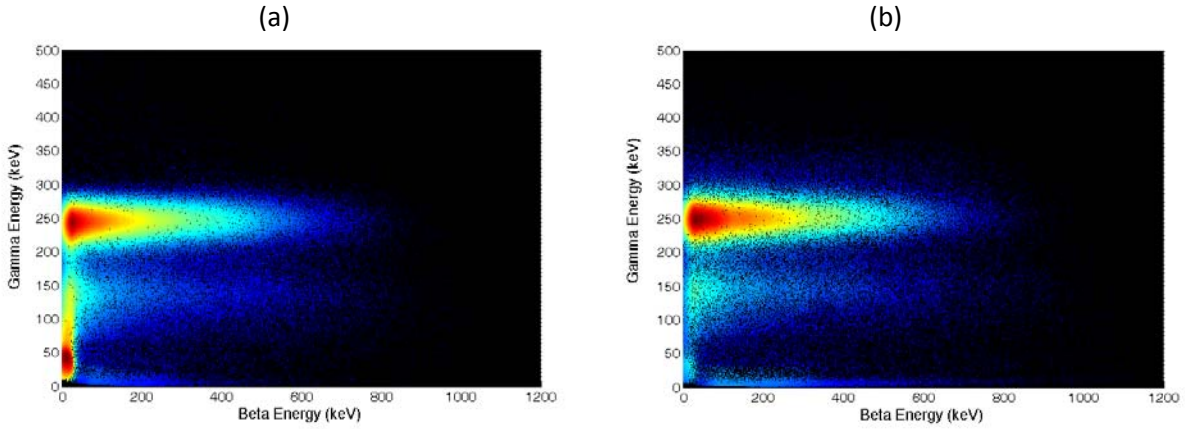

Figure 5. 2-D beta-gamma coincidence energy histograms from ^{135}Xe in channel 1 (a) and channel 2 (b) of the two-channel phoswich detector.

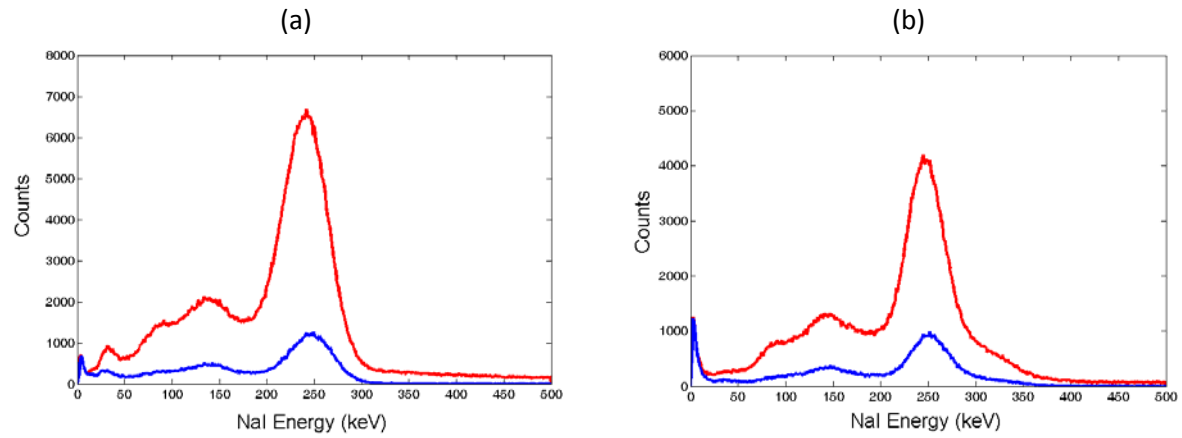

Figure 6. Energy deposition histogram from ^{135}Xe in NaI(Tl) from channel 1 (a) and channel 2 (b) of the two-channel phoswich detector. The red histogram is from NaI(Tl)-only events whereas the blue histogram is from NaI(Tl)-BC400 coincidence events in each channel.

Figure 6 shows the gamma energy deposition in NaI(Tl) from ^{135}Xe in each phoswich channel. The red spectrum is reconstructed from NaI(Tl)-only events. The blue spectrum is also from the NaI(Tl), but when it is in coincidence with an event in the plastic scintillator. The energy resolution of 250 keV from the plastic-NaI(Tl) coincidence histogram was measured to be about 21% for channel 1 and 19% for channel 2. Using the coincidence state machine and synchronizing mode, coincidence events between the two channels were identified and energy histograms (Figure 6) were obtained. Figure 6a shows a 2-D beta-gamma coincidence energy histogram between the two phoswich detectors. This 2-D histogram was updated from single events from both phoswich channels when a coincidence flag was detected by the coincidence state machine. The coincidence window for this experiment was set to 10 clock cycles or 50 nsec. Figure 6b shows a gamma energy histogram from the NaI(Tl) scintillator when a coincidence event was detected between the detectors. The energy resolution of the 250 keV photopeak in this histogram was measured to be 21.6%.

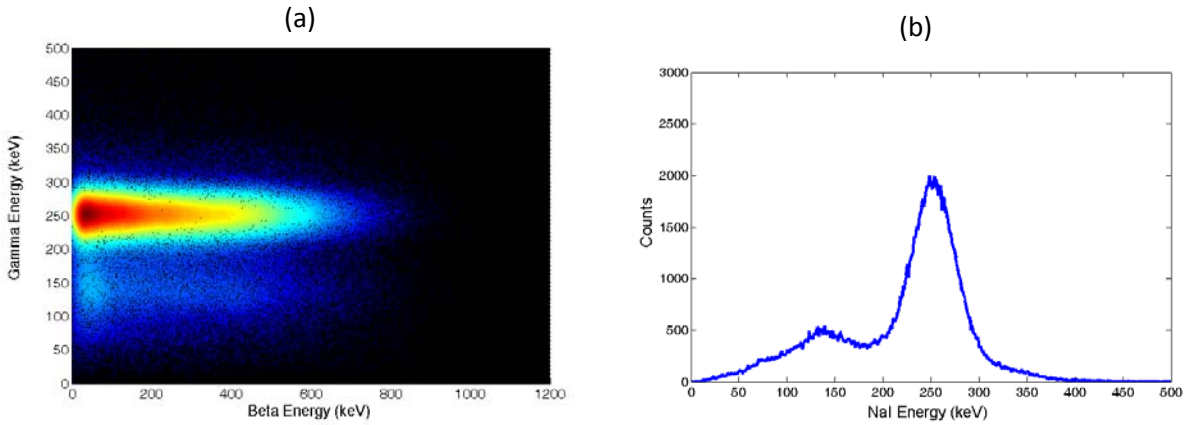

Figure 7. 2-D beta-gamma coincidence energy histogram between the two phoswich detectors (a), and gamma energy histogram from NaI scintillators (b), when the two-channel phoswich detector were exposed to ^{135}Xe.

^{133}Xe and ^{133m}Xe measurements

Three milliliters of enriched and stable ^{132}Xe were irradiated in the thermal column of the TRIGA reactor for 2 hours to produce ^{133}Xe and ^{133m}Xe. Again the thermal neutron flux for this irradiation was $7x10^{10}$ n.cm^{-2}.sec^{-1}. At the end of neutron irradiation, the resulting radioxenon activity was calculated to be around 0.67 and 0.195 µCi for ^{133}Xe and ^{133m}Xe, respectively. An off-line signal processing was then applied on about three million anode pulses from both detectors. Figure 8 shows 2-D beta-gamma coincidence energy spectra collected from both detectors in BC-400/NaI(Tl) after activated xenon gas was injected into the detector gas cell. Horizontal and vertical axes in this figure represent energy absorption in BC-400 and NaI(Tl), respectively. In both channels, 81 keV gamma-ray region is populated with coincidence events. Due to using an optical window (6.35 mm) between NaI (Tl) and CaF_2 crystals, NaI(Tl) crystal was not expected to be as efficient as CaF_2 in detecting 30 keV X-rays. Gamma-ray energy histograms from ^{133}Xe in NaI(Tl) crystal from both channels are depicted in Figure 9. In these histograms, the red histogram is from NaI(Tl)-only events whereas the blue histogram is from NaI(Tl)-BC400 coincidence events. The energy resolution of 81 keV gamma-ray from the plastic-NaI(Tl) coincidence histogram was measured to be about 37% for channel 1 and 26% for channel 2.

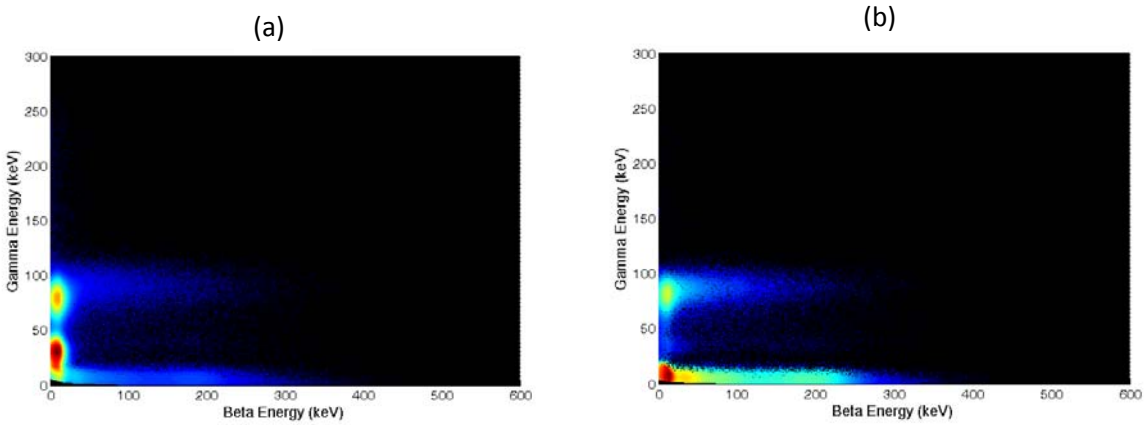

Figure 8. 2-D beta-gamma coincidence energy histograms from ^{133}Xe in channel 1 (a) and channel 2 (b) of the two-channel phoswich detector. Horizontal and vertical axes in this Figure represent energy absorption in BC-400 and NaI(Tl), respectively.

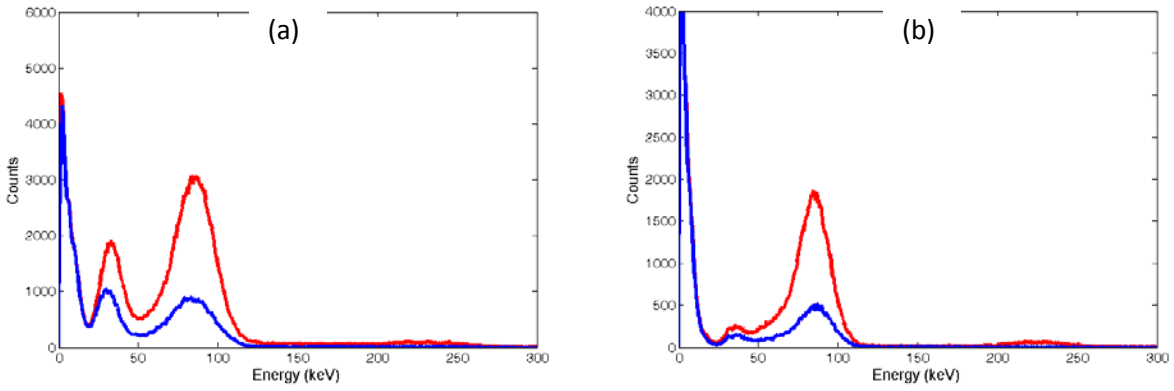

Figure 9. Energy deposition histogram from ^{133}Xe in NaI(Tl) of channel 1 (a) and channel 2 (b) of the two-channel phoswich detector. The red histogram is from NaI(Tl)-only events whereas the blue histogram is from NaI(Tl)-BC400 coincidence events in each channel.

Figure 10 shows 2-D beta-gamma coincidence energy spectra in BC-400/CaF_2 (in channels 1 and 2) when $^{133}Xe/^{133m}Xe$ was injected into the detector gas cell. Due to difficulties in resolving coincidence events from very small pulses (from 30 keV X-rays, see Figure 4) and consequently having poor statistics in energy measurements, the CaF2 spectrum shows a very wide peak for 30 keV X-rays. The corresponding resolution for this peak was measured to be 190% and 200% for channels 1 and 2, respectively. Our previous experiments with a prototype phoswich detector with same design but different PMT (Farsoni et al., 2009) showed a resolution of 43% for 30 keV photopeak in the CaF_2. For both channels, the 2-D coincidence spectrum shows a beta distribution in 30 keV X-ray region. The presence of ^{133m}Xe in the gas sample can be confirmed by observing 199 keV conversion electrons in this region. Beta energy histograms gated with the 30 keV X-ray region from both channels are shown in Figure 11. In each phoswich channel, these histograms were processed from BC-400/CaF_2 coincidence events when a beta event from the plastic is detected in coincidence with 30 keV X-ray from the CaF2. The 30 keV X-ray-gated beta histograms show a peak at 45 keV. This peak represents conversion electrons emitted in coincidence with 30-keV X-rays from ^{133}Xe. In addition, the beta energy histograms in Figure 11 show a peak at about 200 keV. This peak represents 199 keV conversion electrons from ^{133m}Xe when conversion electrons and 30 keV X-rays are detected in coincidence in plastic and CaF_2, respectively.

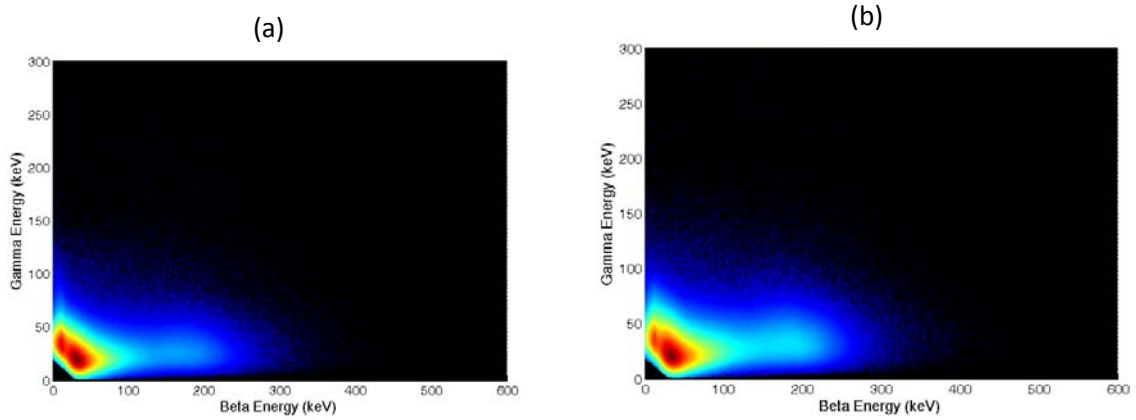

Figure 10. 2-D beta-gamma coincidence energy histograms from $^{133}Xe/^{133m}Xe$ in channel 1 (a) and channel 2 (b) of the two-channel phoswich detector. Horizontal and vertical axes in this Figure represent energy absorption in BC-400 and CaF_2, respectively.

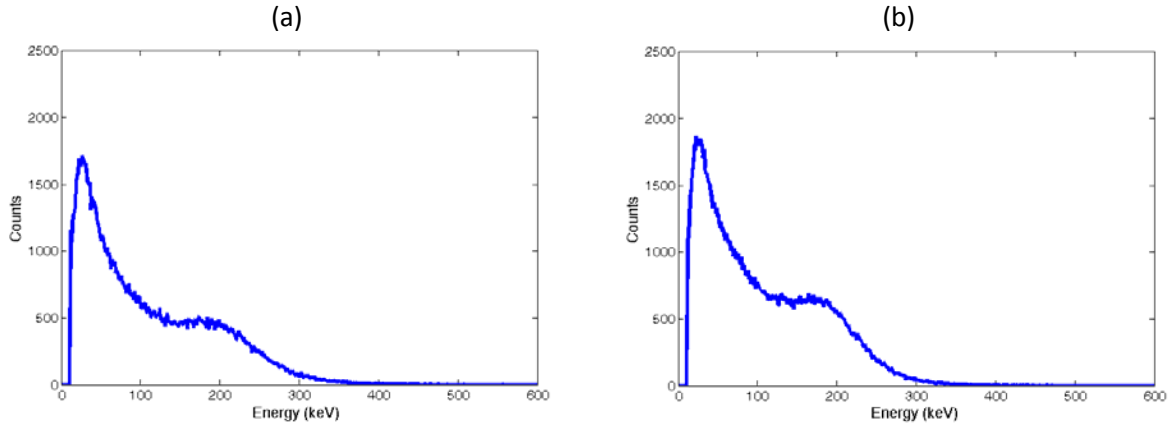

Figure 11. Beta energy histograms (BC-400) from $^{133}Xe/^{133m}Xe$ in plastic scintillator gated with 30-keV X-rays (CaF_2) in channel 1 (a) and channel 2 (b).

CONCLUSION AND RECOMMENDATIONS

In summary, two stable and enriched (>99%) xenon isotopes, ^{134}Xe and ^{132}Xe, were successfully irradiated in the TRIGA reactor to produce xenon radioisotopes ^{135}Xe and ^{133m}Xe and ^{133}Xe for testing a two-channel phoswich detector. Xenon samples in 3-ml polypropylene syringes were irradiated in the thermal column of TRIGA reactor with a thermal neutron flux of $7x10^{10}$ $n.cm^{-2}.sec^{-1}$. A low-cost but efficient gas transfer manifold arrangement was designed to transfer stable xenon gas from its cylinder to a disposable polypropylene syringe and, after neutron irradiation, from there to the detector gas cell. To improve the efficiency of the detection system in capturing coincidence events between the two channels, a synchronizing mode in the FPGA device was designed and characterized. Compared with our prototype detector, the current phoswich-PMT configuration showed a poor energy resolution in detecting 30 keV X-rays with CaF_2 crystal. Use of high-gain PMT's and high-reflective wrapping materials around the phoswich are recommended to improve the resolution.

REFERENCES

Ely, J. H., C. E. Aalseth, J. C. Hayes, T. R. Heimbigner, J. I. McIntyre, H. S. Miley, M. E. Panisko, and M. Ripplinger (2003). Novel Beta-gamma coincidence measurements using phoswich detectors, in *Proceedings of the 25th Seismic Research Review – Nuclear Explosion Monitoring: Building the Knowledge Base*, LA-UR-03-6029, Vol. 2, pp. 533–541.

Farsoni, A. T., D. M. Hamby, K. D. Ropon, and S. E. Jones (2007). A two-channel phoswich detector for dual and triple coincidence measurements of radioxenon isotopes, in *Proceedings of the 29th Seismic Research Review: Ground-Based Nuclear Explosion Monitoring Technologies*, LA-UR-07-5613, Vol. 2, pp. 747–756.

Farsoni, A. T., D. M. Hamby, C. S. Lee, and A. J. Elliott (2008). Preliminary experiments with a triple-layer phoswich detector for radioxenon detection, in *Proceedings of the 2008 Monitoring Research Review: Ground-Based Nuclear Explosion Monitoring Technologies*, LA-UR-08-05261, Vol. 2, pp. 739–748.

Farsoni, A. T., D. M. Hamby (2009). Characterization of triple-layer phoswich detector for radioxenon measurements, in *Proceedings of the 2009 Seismic Research Review: Ground-Based Nuclear Explosion Monitoring Technologies*, LA-UR-09-05276, Vol. 2, pp. 631–640.

Fontaine, J-P., F. Pointurier, X. Blanchard, and T. Taffary (2004). Atmospheric xenon radioactive isotope monitoring, *Journal of Environmental Radioactivity* 72: 129–135

Hennig, W., H. Tan, W. K. Warburton, and J. I. McIntyre (2005). Digital pulse shape analysis with phoswich detectors to simplify coincidence measurements of radioactive xenon, in *Proceedings of the 27th Seismic Research Review: Ground-Based Nuclear Explosion Monitoring Technologies,* LA-UR-05-6407, Vol. 2, pp. 787–794.

McIntyre, J. I., K. H. Able, T. W. Bowyer, J. C. Hayes, T. R. Heimbigner, M. E. Panisko, P. L. Reeder, and R. C. Thompson (2001). Measurements of ambient radioxenon levels using the automated radioxenon sampler/analyzer (ARSA), *J. Radioanal. Nucl. Chem*. 248: 629–635.

Ringbom, A., T. Larson, A. Axelson, K. Elmgren, and C. Johonson (2003). SAUNA - a system for automatic sampling, processing and analysis of radioactive xenon, *Nuclear Instruments and Methods in Physics Research* A 508: 542–553.

Seifert, C. E., J. I. McIntyre, K. C. Antolick, A. J. Carman, M.W. Cooper, J. C. Hayes, T. R. Heimbigner, C. W. Hubbard, K. E. Litke, M. D. Ripplinger, and R. Suarez (2005). Mitigation of memory effects in beta scintillation cells for radioactive gas detection, in *Proceedings of the 27th Seismic Research Review – Nuclear Explosion Monitoring Technologies,* LA-UR-05-6407, Vol. 2, pp. 804–814.